

See discussions, stats, and author profiles for this publication at: <https://www.researchgate.net/publication/231398401>

Analysis of long-range dispersion and exchange interactions of two lithium atoms

ARTICLE *in* THE JOURNAL OF PHYSICAL CHEMISTRY · MARCH 1993

Impact Factor: 2.78 · DOI: 10.1021/j100112a001

CITATIONS

35

READS

25

2 AUTHORS:



Warren Zemke

Wartburg College

64 PUBLICATIONS 1,244 CITATIONS

SEE PROFILE



William C Stwalley

University of Connecticut

425 PUBLICATIONS 7,348 CITATIONS

SEE PROFILE

Analysis of long range dispersion and exchange interactions between two K atoms

Warren T. Zemke

Department of Chemistry, Wartburg College, Waverly, Iowa 40677

Chin-Chun Tsai and William C. Stwalley^{a)}

Department of Physics and Institute of Materials Science, University of Connecticut, Storrs, Connecticut 06269-3046

(Received 2 August 1994; accepted 6 September 1994)

This paper critically surveys the best available spectroscopic data for the two lowest electronic states ($X^1\Sigma_g^+$ and $a^3\Sigma_u^+$) of K_2 . Since both states are known up to dissociation, they can be used to determine Coulomb and exchange contributions to the intermediate and long range interaction potentials. The multipolar expansion representation of the Coulomb (dispersion) energy at long range ($-\Sigma_n C_n R^{-n}$) and the exponential representation of the exchange energy ($Ae^{-\alpha R}$) as well as a variety of theoretical calculations are compared with these empirical results. Finally, dissociation energy values are discussed and improved dissociation energies for the $X^1\Sigma_g^+$ ($D_e=4449.1\pm 1.0$ cm⁻¹) and the $a^3\Sigma_u^+$ state ($D_e=252.9\pm 1.1$ cm⁻¹) proposed. © 1994 American Institute of Physics.

I. INTRODUCTION

The two lowest electronic states of K_2 ($X^1\Sigma_g^+$ and $a^3\Sigma_u^+$) dissociate to the same asymptotic limit, two ground state $4s^2S$ atoms. If the potential curves of both molecular states are known precisely up to near dissociation (see Fig. 1), they can be used to determine Coulomb and exchange energies as a function of internuclear distance R . This provides a direct empirical determination for the description of covalent chemical bonding in terms of the fundamental concepts of electronic Coulomb (dispersion) and exchange contributions. This type of analysis has previously been applied to the case of two $Li(2s)$ atoms¹ and two $Na(3s)$ atoms.²

At long range where the atomic overlap is small, the potential energies $\Delta V_X(R)$ and $\Delta V_a(R)$ with respect to dissociation [i.e., $\Delta V_X(\infty)=\Delta V_a(\infty)=0$] can be described in terms of the Coulomb contribution ΔV_C (dispersion) and the exchange contribution ΔV_E . In particular

$$\Delta V_X(R) = \Delta V_C(R) + \Delta V_E(R)$$

and

$$\Delta V_a(R) = \Delta V_C(R) - \Delta V_E(R),$$

where it might be noted that both ΔV_C and ΔV_E are negative quantities. Alternatively, one can readily determine the values of ΔV_C and ΔV_E from the sum and difference of the (empirical) potentials,

$$\Delta V_C(R) = 1/2[\Delta V_X(R) + \Delta V_a(R)],$$

$$\Delta V_E(R) = 1/2[\Delta V_X(R) - \Delta V_a(R)].$$

In the literature, of course, potentials are often given with respect to the potential minimum, not the separated atom (dissociation) limit, i.e., $V(R)=D_e+\Delta V(R)$. Thus one obtains

$$\Delta V_C = 1/2(V_X + V_a) - D_e,$$

$$\Delta V_E = 1/2(V_X - V_a).$$

Two simple analytical representations for these energy contributions are the second-order long range multipolar expansion in terms of separated atoms³

$$\Delta V_C^{(2)\infty}(R) = -C_6 R^{-6} - C_8 R^{-8} - C_{10} R^{-10} - \dots$$

and the exponential⁴

$$\Delta V_E(R) = Ae^{-\alpha R},$$

which vanishes rapidly at very large R . We will compare these approximations and also a variety of other theoretical results with our empirical results, as previously done for Li_2 and Na_2 .^{1,2} It might be noted that hyperfine structure is ignored, but it should only be important at distances much greater than those considered here.

Our procedure is as follows. In Secs. II and III we describe the spectroscopic data and the hybrid potential curves for the $X^1\Sigma_g^+$ and $a^3\Sigma_u^+$ states of K_2 , respectively. In Secs. IV and V we determine and discuss the long-range Coulomb and exchange interactions, respectively. In Sec. VI we describe dissociation energy estimates and recommend an improved value. Conclusions are presented in Sec. VII.

II. THE $X^1\Sigma_g^+$ STATE

From laser-induced spectroscopic studies of the $A^1\Sigma_u^+ \rightarrow X^1\Sigma_g^+$ and $B^1\Pi_u \rightarrow X^1\Sigma_g^+$ systems, Amiot⁵ was able to construct a ground state potential energy curve that goes up to within 0.7% of the dissociation limit, two $K(4s)$ atoms. Amiot recorded more than 3000 rovibrational transitions by Fourier transform infrared (FTIR) spectroscopy. Because of the extent and high resolution (≈ 0.004 cm⁻¹) of his data, we consider this inverse perturbation analysis (IPA) potential energy curve the best experimental curve available.

Since there is a paucity of information characterizing the uppermost portion of the inner wall of the ground state, we fit the innermost turning points of the IPA curve to obtain an

^{a)}Also Department of Chemistry.

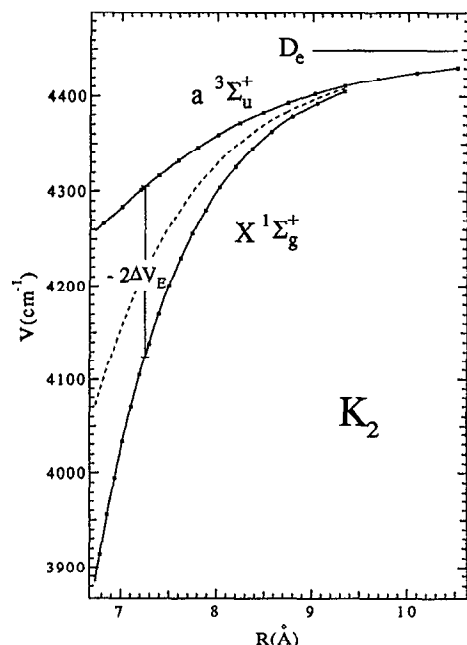


FIG. 1. Long range regions of the experimentally-based curves for the $X\ ^1\Sigma_g^+$ and $a\ ^3\Sigma_u^+$ states of K_2 . The dashed line is D_c plus the (negative) Coulomb energy ΔV_C . The splitting between the X and a state energies is twice the exchange energy ($-2\Delta V_E$). $D_c=4449.1\pm 1.0\text{ cm}^{-1}$. The $a\ ^3\Sigma_u^+$ state RKR potential shown is given with respect to the $X\ ^1\Sigma_g^+$ state minimum [i.e., $T_e(a\ ^3\Sigma_u^+) + V_a(R)$].

exponential function Be^{-bR} which permits us to extrapolate the ground state well above the dissociation limit [see Table I (X state, region I) for the exact exponential].

The long-range portion of the ground state curve (beyond the last Amiot turning point $R_{73+}=9.335\text{ Å}=17.64\text{ }a_0$) is best represented by the dispersion coefficients of Marinescu *et al.*⁶ and exchange energy exponential based on the *ab initio* calculations of Magnier.⁷ The long range portion of the ground state hybrid potential energy curve is fully described in Table I (region III).

The theoretical dispersion (van der Waals) coefficients for the $X\ ^1\Sigma_g^+$ state (and the $a\ ^3\Sigma_u^+$ state) of K_2 are given in Table II. The most precise calculations for C_6 in our opinion are those of Marinescu *et al.*,⁶ which are coincidentally very close to the average (3803 a.u.) of other results (excluding Busser and Aubert-Frecon¹⁵). Moreover, the Marinescu *et al.* calculations have been slightly scaled to agree exactly with the experimental dipole polarizability ($292.8\pm 6.1\text{ }a_0^3$) of Molof *et al.*¹⁸ Since the uncertainty in the dipole polarizability is the dominant uncertainty in the C_6 value, we estimate $\Delta C_6/C_6 \approx 2\Delta\alpha/\alpha = 0.042$ or $C_6=3813\pm 160\text{ a.u.}$ Probably the next most accurate result is the work of Spelsberg *et al.*;¹⁶ if that result is scaled using the experimental dipole polarizability, one obtains $C_6=3809$, in excellent agreement with the Marinescu *et al.* value. Uncertainties of $\sim 4\%$ are assumed in C_8 and C_{10} values as well as C_6 . Experimental estimates of C_6 , C_8 , and C_{10} by Amiot⁵ are not considered to be comparably reliable. In particular, those estimates vary considerably within the paper and are based on $X\ ^1\Sigma_g^+$ internuclear distances $R < R_{73+}=9.335\text{ Å}$, well inside the K_2

TABLE I. Hybrid potential energy curves for the $X\ ^1\Sigma_g^+$ and $a\ ^3\Sigma_u^+$ states of K_2 .

Region	Range of R (Å)	$V(R)$ function (cm^{-1}) ^a
X state		
I	$R \leq 2.870\ 683\ 0$	Be^{-bR} ^b
II	$2.870\ 683\ 0 \leq R \leq 10.054\ 367\ 7$	Tensioned cubic spline fit to the IPA points of Table III in Ref. 5 and the long range point at $10.054\ 367\ 7\text{ Å}$ ($19\text{ }a_0$).
III	$10.054\ 367\ 7 \leq R$	$D_c - C_6/R^6 - C_8/R^8 - C_{10}/R^{10} - Ae^{-aR}$ ^c
a state		
I	$R \leq 4.823\ 883\ 4$	Tensioned cubic spline fit of scaled <i>ab initio</i> points fitted to R_{17-} .
II	$4.823\ 883\ 4 \leq R \leq 10.583\ 545\ 0$	Tensioned cubic spline fit to the RKR points of Ref. 20 and the point at $10.583\ 545\ 0\text{ Å}$ ($20\text{ }a_0$). ^e
III	$10.583\ 545\ 0 \leq R$	$D_c - C_6/R^6 - C_8/R^8 - C_{10}/R^{10} + Ae^{-aR}$ ^c

^a $V(R)$ is in cm^{-1} with respect to the minimum of the ground state curve; R is in Å units. $V(R)$ and dV/dR are continuous.

^b $B=3.046\ 569\ 4 \times 10^6\text{ cm}^{-1}$ and $b=2.277\ 876\text{ (Å)}^{-1}$ based on a fit to $R_{69}=R_{73-}$ points of Ref. 5.

^c $D_c=4449.1\text{ cm}^{-1}$ (see text); $C_6=1.837\ 63 \times 10^7\text{ cm}^{-1}(\text{Å})^6$, $C_8=5.527\ 82 \times 10^8\text{ cm}^{-1}(\text{Å})^8$, $C_{10}=1.983\ 31 \times 10^{10}\text{ cm}^{-1}(\text{Å})^{10}$ (see Table II); $A=5.632\ 963\ 2 \times 10^6\text{ cm}^{-1}$, $\alpha=1.524\ 132\text{ (Å)}^{-1}$.

^dThe inner wall points of Ref. 7 (from 5.0 to 9.0) plus the interpolated point at $R_{17-}=9.115\ 817\ 8\text{ Å}$, $a_0=4.823\ 883\ 4\text{ Å}$ are scaled to fit the RKR R_{17-} point by adding $7.504\ 25\text{ cm}^{-1}$ to them.

^eTurning points (but not the G_v+Y_{00} values) for $v=14-17$ levels from Table VII in Ref. 20 have been slightly shifted to $R_{14-}=4.858\ 054\ 0$, $R_{14+}=9.340\ 065\ 0$, $R_{15-}=4.844\ 776\ 1$, $R_{15+}=9.686\ 580\ 5$, $R_{16-}=4.833\ 427\ 9$, $R_{16+}=10.091\ 037\ 0$, $R_{17-}=4.823\ 883\ 4$, $R_{17+}=10.515\ 443\ 3$ (see text).

“LeRoy radius” of 10.775 Å (Ref. 19) inside which exchange is expected to be important. In addition, the dissociation energy found by Amiot⁵ is significantly higher than that found here (see Sec. VI).

The complete $X\ ^1\Sigma_g^+$ state potential energy curve is a hybrid potential described in Table I. Eigenvalue calculations were performed with the hybrid potential. The calculated energies showed self-consistency of the $G(v)+Y_{00}$ energies⁵ used to construct the potential; for all $v=0-73$ levels, no difference exceeded 0.14 cm^{-1} and the standard deviation was 0.06 cm^{-1} .

III. THE $a\ ^3\Sigma_u^+$ STATE

The perturbation facilitated optical-optical double resonance spectroscopic studies of Li *et al.*²⁰ yielded resolved fluorescence spectra to the $a\ ^3\Sigma_u^+$ state which, in turn, yielded an a state potential energy curve that covered nearly 93% of the well.

With the very recent $a\ ^3\Sigma_u^+$ state calculations of a very complete potential curve⁷ and more accurate C_n dispersion coefficients⁶ (Li *et al.* used earlier less reliable values from Refs. 9 and 15), we were able to construct a new and improved hybrid potential energy curve. The approach used for the construction of the a state hybrid potential is similar to that used for the X state hybrid potential; region II (the well)

TABLE II. Dispersion coefficients (in atomic units^a) for the $X\ ^1\Sigma_g^+$ and $a\ ^3\Sigma_u^+$ states of K_2 .

Reference	C_6	C_8	C_{10}
Dalgarno ^c	3820		
Dalgarno and Davison ^d	4100		
Dalgarno and Davison ^e	3680		
Tang, Norbeck, and Certain ^f	3890	446 000	54 900 000
Maeder and Kutzelnigg ^g	3945	383 400	45 220 000
Müller, Flesch, and Meyer ^h	3574		
Manakov and Ovsiannikov ⁱ	3780		
Bussery and Aubert-Frecon ^j	4721	389 400	40 690 000
Spelsberg, Lorenz, and Mayer ^{b,k}	3637	401 100	54 310 000
Marinescu, Sadeghpour, and Dalgarno ^l	3813	409 600	52 480 000
Recommended (used in this work)	3813	409 600	52 480 000
	± 160	$\pm 16\ 000$	$\pm 2\ 000\ 000$

^aThus C_6 is in hartree a_0^6 . Conversions to cm^{-1} and a_0 are $1\ a_0 = 0.529\ 177\ 249\ \text{\AA}$ and $1\ \text{hartree} = 219\ 474.631\ 418\ \text{cm}^{-1}$ (Ref. 17).

^bAlso $C_{12} = 1.571 \times 10^{10}\ \text{a.u.}$

^cReference 8.

^dReference 9.

^eReference 10.

^fReference 11.

^gReference 12.

^hReference 13.

ⁱReference 14.

^jReference 15.

^kReference 16.

^lReference 6.

of the potential is based on the best available RKR curve²⁰ and region III (the long range portion) is based on the dispersion coefficients of Marinescu *et al.*⁶ and the exchange energy exponential based on the *ab initio* calculations of Magnier⁷ (see Table I).

The Li *et al.*²⁰ RKR curve was adjusted at the four uppermost observed levels ($v=14-17$) because of "inner wall bending."²⁰ The adjustment was in part based on the *ab initio* $a\ ^3\Sigma_u^+$ state potential energy curve of Krauss and Stevens,²¹ with a particular emphasis on the upper inner wall. We found that their minor adjustments in the upper RKR levels were overdone. The inner slopes of much of the RKR curve (region II, Table I) and the theoretical Magnier⁷ curve are amazingly parallel, except the points where Li *et al.*²⁰ made adjustments. To correct this, we shifted the uppermost ($v=14-17$) turning points to slightly smaller distances, in harmony with the *ab initio* slope.⁷

The shift in the innermost part of region II resulted in an accompanying shift in the outermost part of region II, based on the fact that the difference $R_{v+} - R_{v-}$ is more reliably determined than either R_{v+} or R_{v-} separately. For a complete rationale of this point, see the papers by LeRoy¹⁹ and Yang.²² See footnote e of Table I for exact R_{v-} and R_{v+} values for $v=14-17$.

Region I of the $a\ ^3\Sigma_u^+$ state hybrid potential is the inner wall of the Magnier⁷ *ab initio* potential, scaled to fit continuously on the innermost R_{17-} turning point (see Table I).

The complete $a\ ^3\Sigma_u^+$ state potential energy curve is a hybrid potential described in Table I. Eigenvalue calculations with this hybrid potential were compared with the $G(v) + Y_{00}$ values of Li *et al.*²⁰ Agreement was quite satisfactory; no difference exceeded $0.05\ \text{cm}^{-1}$ and the standard deviation for all $v=0-17$ levels was $0.03\ \text{cm}^{-1}$.

IV. COULOMB ENERGY

The Coulomb energies at various internuclear distances determined herein using the equation

$$\Delta V_C(R) = 1/2[V_X(R) + V_A(R)] - D_e$$

are given in Table III and plotted in Fig. 2. For comparison, the expansion

$$\Delta V_C^{(2)}(R) = -C_6 R^{-6} - C_8 R^{-8} - C_{10} R^{-10}$$

with the dispersion coefficients of Marinescu *et al.*⁶ (Sec. II) is also given and plotted. The agreement between these re-

TABLE III. Coulomb energies, $-\Delta V_C$ (cm^{-1}), for K_2 .

R		Experiment (this work ^a)	<i>ab initio</i>		Expanded power series (Ref. 6 ^b)
a_0	\AA		Ref. 7 ^a	Ref. 23 ^a	
11.5	6.086	676.76	631.98		940.38
12.0	6.350	535.00	497.44	771.45	675.36
13.0	6.879	329.58	304.96	503.69	367.13
14.0	7.408	203.06	189.52	324.82	211.88
15.0	7.938	126.99	121.70	212.89	128.52
16.0	8.467	81.25	81.32		81.29
17.0	8.996	53.37	56.30		53.27
17.64 ^c	9.335	41.19	45.34 ^d		41.29
18.0	9.525		40.38		35.99
19.0	10.054		29.74		24.96
20.0	10.584		22.50		17.71
22.0	11.642		13.72		9.45

^a $\Delta V_C = 1/2(V_X + V_A) - D_e$.

^b $\Delta V_C = -C_6/R^6 - C_8/R^8 - C_{10}/R^{10}$, where C_n coefficients are tabulated in Table II.

^cThe $v''=73$ outer turning point for the $X\ ^1\Sigma_g^+$ state, Ref. 5.

^dInterpolated.

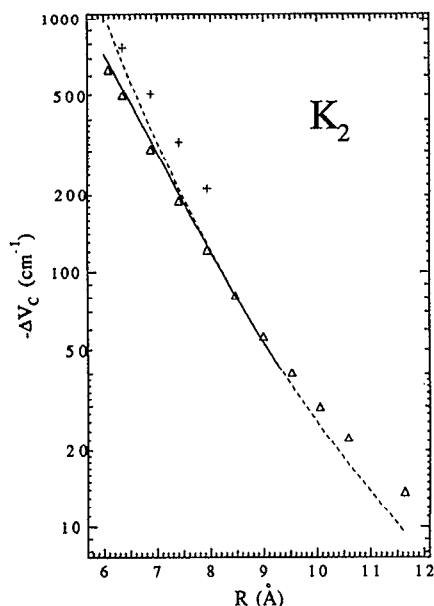


FIG. 2. Magnitude of the empirical Coulomb energy $-\Delta V_C$ (cm^{-1}) in the region 6–9.3 Å is indicated by the solid line. The expanded dispersion energy ($\Delta V_C = -\sum_n C_n/R^n$) is based on the C_n coefficients of Ref. 6 (see Table II) and indicated by the dashed line from 6 to 11.6 Å. *Ab initio* ΔV_C values are those of Ref. 7 (Δ) and Ref. 23 (+). See also Table III.

sults is remarkably good outside ~ 8 Å. Inside ~ 8 Å, the experimental magnitude of the ΔV_C is “damped” by overlap effects compared to the inverse R expansion, as previously discussed for Li_2 .¹ Note also that the distance of ~ 8 Å where Coulomb overlap effects occur in ΔV is well inside the 10.775 Å distance (“LeRoy radius,” Ref. 19) where overlap exchange effects occur.

The theoretical $X^1\Sigma_g^+$ and $a^3\Sigma_u^+$ potential curves of Magnier⁷ and Jeung and Ross²³ can also be used to compute ΔV_C (Table III; Fig. 2), although the number of significant figures in Ref. 7 limit the accuracy at the larger distances. It is clear that the agreement with experiment is very good for the calculations of Magnier⁷ and somewhat less good for the calculations of Jeung and Ross.²³

V. EXCHANGE ENERGY

The exchange energies at various internuclear distances determined herein using the equation

$$\Delta V_E(R) = 1/2[V_X(R) - V_a(R)]$$

are given in Table IV and plotted in Fig. 3. Note that, as previously found for Li_2^1 and Na_2^2 , the decay of ΔV_E with increasing R is very nearly exponential. The dashed line in Fig. 3 is an exponential fit to several *ab initio* ΔV_E points based on Magnier.⁷ It does appear that $\Delta V_E(R)$ falls below the exponential significantly at shorter R and also at larger R . Again the results of Jeung and Ross²³ deviate more significantly from our experimental results than those of Magnier.⁷

TABLE IV. Exchange energies, $-\Delta V_E$ (cm^{-1}), for K_2 .

a_0	R Å	Experiment (this work ^a)	<i>ab initio</i>		Exponential fit (Ref. 7 ^b)
			Ref. 7 ^a	Ref. 23 ^a	
11.5	6.086	434.21	412.06		527.94
12.0	6.350	311.20	295.96	418.10	352.73
13.0	6.879	152.81	146.50	222.77	157.46
14.0	7.408	71.75	69.46	111.93	70.29
15.0	7.938	32.52	31.93	54.87	31.38
16.0	8.467	14.19	14.38		14.01
17.0	8.996	5.89	6.26		6.25
17.64 ^c	9.335	3.22	3.76 ^d		3.73
18.0	9.525		2.85		2.79
19.0	10.054		1.21		1.25
20.0	10.584		0.55		0.56
22.0	11.642		0.11		0.11

^a $\Delta V_E = 1/2(V_X - V_a)$.

^b $\Delta V_E = -Ae^{-\alpha R}$, based on a fit to the eight *ab initio* points from 14 to 22 a_0 ; $A = 25.665\,669$ hartrees and $\alpha = 0.806\,536\,a_0^{-1}$.

^cThe $v''=73$ outer turning point for the $X^1\Sigma_g^+$ state, Ref. 5.

^dInterpolated.

VI. DISSOCIATION ENERGY

The dissociation energy values of the $X^1\Sigma_g^+$ and $a^3\Sigma_u^+$ states of K_2 were recently reviewed by Li *et al.*,²⁰ who recommended $D_e'' = D_e(X^1\Sigma_g^+) = 4450 \pm 2\text{ cm}^{-1}$ and $D_e(a^3\Sigma_u^+) = 254 \pm 2\text{ cm}^{-1}$. However, the more recent work of Amiot⁵ and this work provide additional information which can be used to estimate improved D_e values. These new results are summarized in Fig. 4.

Amiot⁵ in four different ways estimated D_e values between 4449.7 and 4455 cm^{-1} ; he concluded by recommend-

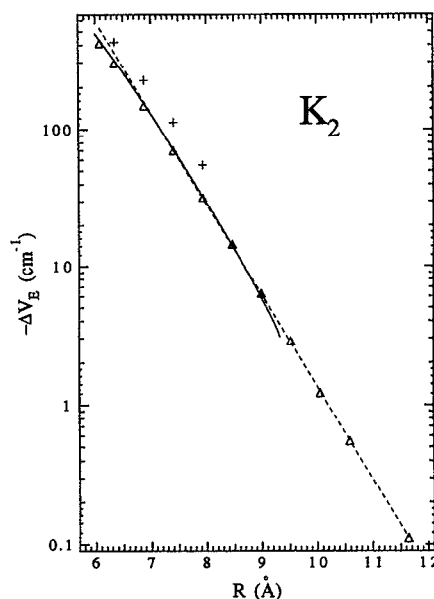


FIG. 3. Magnitude of the empirical exchange energy $-\Delta V_E$ (cm^{-1}) in the region of 6–9.3 Å is indicated by the solid line. The dashed line is our exponential fit to the *ab initio* points of Magnier (Ref. 7) from 7.5 to 11.6 Å. The *ab initio* ΔV_E values are those of Ref. 7 (Δ) and Ref. 23 (+). See also Table IV.

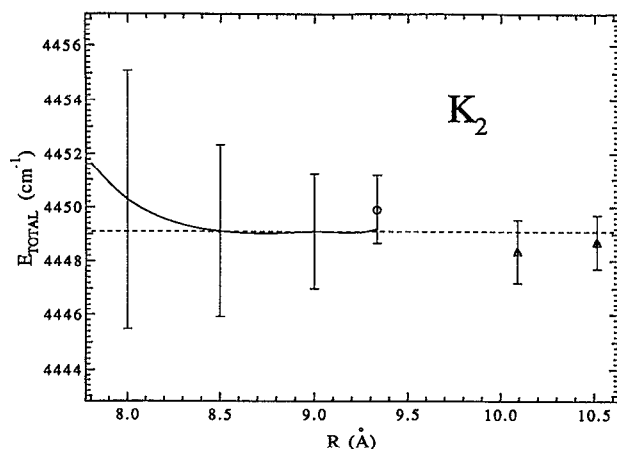


FIG. 4. Estimates of the dissociation energy D_e'' of the $X^1\Sigma_g^+$ state of K_2 . The solid curve (with occasional error bars) represents the sum of the dispersion potential $[1/2(V_X + V_A)]$ plus $-\Delta V_C(+C_6R^{-6} + C_8R^{-8} + C_{10}R^{-10})$ and should equal D_e'' when overlap damping is unimportant (outside 8.5 Å in the plot). The point at $R_{73+}=9.335$ Å (0 with error bars) is based on the RKR curve of Ref. 5 for the $X^1\Sigma_g^+$ state. The points at $R_{16+}=10.091$ Å and $R_{17+}=10.515$ Å (Δ with error bars) is based on our new curve for the $a^3\Sigma_u^+$ state, which is based on the data of Ref. 20. Our overall recommended D_e'' value, based primarily on the solid curve, is 4449.1 ± 1.0 cm^{-1} (dashed line).

ing $D_e=4451 \pm 1.5$ cm^{-1} . In our opinion, the most accurate estimate of D_e'' based on his data alone would be that for R_{73+} as shown in Table V ($D_e'' = 4449.9 \pm 1.8$ cm^{-1}), where the uncertainty in ΔV_C is taken as 4% and in ΔV_E as 5%.

The same approach applied to the data of Li *et al.*²⁰ alone is also shown in Table VI and Fig. 4. The most accurate estimate would be that based on R_{17+} ($D_e'' = 4448.7 \pm 1.0$ cm^{-1}). Note that $R_{17+}(a)=10.514$ Å $\gg R_{73+}(X)=9.35$ Å, so the $a^3\Sigma_u^+$ value is derived from data at longer range and is thus less uncertain (although this is particularly offset by the higher precision of Amiot's FTIR spectra⁵ compared to the spectrally resolved fluorescence of Li *et al.*²⁰).

However, the consideration of both $X^1\Sigma_g^+$ and $a^3\Sigma_u^+$ data simultaneously (i.e., through determination of V_C) al-

TABLE V. Energy contributions and totals (each in cm^{-1}) at specific RKR outer turning points (R in Å) in the $K_2 X^1\Sigma_g^+$ ground electronic state.

	$v=70$	$v=71$	$v=72$	$v=73$
R^a	8.5739	8.7968	9.0486	9.3353 ± 0.001
$V(R)^b$	4362.729	4378.596	4392.634	4404.877 ± 0.004
$-\Delta V_C^c$	74.426	62.218	51.167	41.293 ± 1.65
$-\Delta V_E^d$	11.898	8.471	5.771	3.728 ± 0.19
E_{total}^e	4449.053	4449.284	4449.571	4449.898 ± 1.84^f

^a R values are the outermost RKR turning points from Ref. 5.

^b $V(R)=G(v)+Y_{00}$, Ref. 5.

^c $-\Delta V_C(R)=\sum C_n/R^n$, using C_n coefficients from Ref. 6.

^d $-\Delta V_E(R)=Ae^{-\alpha R}$, based on our fit to the *ab initio* $\Delta V_E=1/2(V_X-V_A)$ values, Ref. 7.

^e $E_{\text{total}}=V(R)-\Delta V_C(R)-\Delta V_E(R)$.

^f0.04 of the total 1.84 cm^{-1} uncertainty is because of the uncertainty in R .

lows a third determination of D_e'' , namely 4449.1 ± 1.0 cm^{-1} , based on the dotted curve in Fig. 4. In particular, ΔV_C should be accurately described by $\Delta V_C^{(2)\infty}$ well inside the LeRoy radius, since the exchange ΔV_E interaction cancels out. The dominant uncertainty in this D_e'' (as noted in Sec. II) is due to the uncertainty in C_6 (and hence in α_K). The excellent agreement among the X , a , and combined D_e'' values suggests a recommended value of 4449.1 ± 1.0 cm^{-1} . This is inside the earlier²⁰ 4450 ± 2 cm^{-1} bounds and suggests both the C_6 and α_K values may in fact be less uncertain than is quoted above.

Finally, we note the corresponding value for $D_0''=D_0(X^1\Sigma_g^+)=4449.1-46.1=4403.0 \pm 1.0$ cm^{-1} , and for the $a^3\Sigma_u^+$ state, $D_e''(a^3\Sigma_u^+)=D_e''-T_e(a^3\Sigma_u^+)=252.9 \pm 1.1$ cm^{-1} and $D_0''(a^3\Sigma_u^+)=252.9-10.7=242.2 \pm 1.2$ cm^{-1} .

VII. CONCLUSIONS

Our recommended $X^1\Sigma_g^+$ and $a^3\Sigma_u^+$ potential energy curves for K_2 have been combined to empirically determine Coulomb energies, exchange energies, and dissociation energies. These results strongly support the high quality of dispersion calculations (e.g., by Marinescu *et al.*⁶) and of molecular electronic structure calculations (e.g., by Magnier⁷).

TABLE VI. Energy contributions and totals (each in cm^{-1}) at specific RKR outer turning points (R in Å) in the $K_2 a^3\Sigma_u^+$ electronic state.

	$v=14$	$v=15$	$v=16$	$v=17$
R^a	9.340	9.687	10.091 ± 0.02	10.515 ± 0.03
$V(R) + T_e^b$	4411.05	4418.58	4425.18 ± 0.13	4430.83 ± 0.13
$-\Delta V_C^c$	41.15	32.10	24.36 ± 0.93	18.49 ± 0.81
ΔV_E^d	-3.70	-2.18	-1.18 ± 0.10	-0.62 ± 0.06
E_{total}^e	4448.50	4448.51	4448.36 ± 1.16^f	4448.70 ± 1.00^g

^a R values are the outermost RKR turning points from Ref. 20; these points have been shifted to slightly shorter distances (see text).

^b $V(R)=G(v)+Y_{00}$ and $T_e=4196.1587$ cm^{-1} from Ref. 20.

^c $-\Delta V_C(R)=\sum C_n/R^n$, using C_n coefficients from Ref. 6.

^d $-\Delta V_E(R)=Ae^{-\alpha R}$, based on our fit to the *ab initio* points of Ref. 7.

^e $E_{\text{total}}=V(R)+T_e-\Delta V_C(R)+\Delta V_E(R)$.

^f0.36 of the total 1.16 cm^{-1} uncertainty is because of uncertainty in R .

^g0.38 of the total 1.00 cm^{-1} uncertainty is because of uncertainty in R .

Such high accuracy at long-range is critical to understanding collisions of ultracold atoms (see e.g., Ref. 24, and references therein).

ACKNOWLEDGMENTS

Helpful discussions with G. Jeung, F. Masnou-Seeuws, and A. Dalgarno are gratefully acknowledged, as is the support received from the National Institute of Standards and Technology and the National Science Foundation.

¹W. T. Zemke and W. C. Stwalley, *J. Phys. Chem.* **97**, 2053 (1993).

²W. T. Zemke and W. C. Stwalley, *J. Chem. Phys.* **100**, 2661 (1994).

³J. O. Hirschfelder and W. J. Meath, *Adv. Chem. Phys.* **12**, 3 (1967).

⁴E. A. Mason and L. Monchick, *Adv. Chem. Phys.* **12**, 329 (1967).

⁵C. Amiot, *J. Mol. Spectrosc.* **146**, 370 (1991).

⁶M. Marinescu, H. R. Sadeghpour, and A. Dalgarno, *Phys. Rev. A* **49**, 982 (1994).

⁷S. Magnier, Ph.D. thesis, University of Paris, Orsay, France, 1993.

⁸A. Dalgarno, *Adv. Chem. Phys.* **12**, 143 (1967).

⁹A. Dalgarno and W. D. Davison, *Mol. Phys.* **13**, 479 (1967).

¹⁰A. Dalgarno and W. D. Davison, *Adv. At. Mol. Phys.* **2**, 1 (1966).

¹¹K. T. Tang, J. M. Norbeck, and P. R. Certain, *J. Chem. Phys.* **64**, 3063 (1976).

¹²F. Maeder and W. Kutzelnigg, *Chem. Phys.* **42**, 95 (1979).

¹³W. Müller, J. Flesch, and W. Meyer, *J. Chem. Phys.* **80**, 3297 (1984).

¹⁴M. L. Manakov and V. O. Ovsiannikov, *J. Phys. B* **10**, 569 (1985).

¹⁵B. Bussery and M. Aubert-Frecon, *J. Chem. Phys.* **82**, 3224 (1985).

¹⁶D. Spelsberg, T. Lorenz, and W. Meyer, *J. Chem. Phys.* **99**, 7845 (1993).

¹⁷E. R. Cohen and B. N. Taylor, *Rev. Mod. Phys.* **59**, 1121 (1987).

¹⁸R. W. Molof, H. L. Schwartz, T. M. Miller, and B. Bederson, *Phys. Rev. A* **10**, 1131 (1974).

¹⁹R. J. LeRoy, in *Specialist Periodical Reports, Molecular Spectroscopy* (Chemical Society, London, 1973), Vol. 1, p. 113.

²⁰L. Li, A. M. Lyyra, W. T. Luh, and W. C. Stwalley, *J. Chem. Phys.* **93**, 8452 (1990).

²¹M. Krauss and W. J. Stevens, *J. Chem. Phys.* **93**, 4236 (1990).

²²S. C. Yang, *J. Chem. Phys.* **77**, 2884 (1982).

²³G.-H. Jeung and A. J. Ross, *J. Phys. B* **21**, 1473 (1988).

²⁴A. J. Moerdijk, W. C. Stwalley, R. G. Hulet, and B. J. Verhaar, *Phys. Rev. Lett.* **72**, 40 (1994).